then with a gradient to 90 percent for 15 minutes. One of the peaks eluted with synthetic octacosa somatostatin after 35 minutes. The other peak eluted earlier and was tentatively identified, by its similar molecular size, as somatostatin-25 (4-28 octacosa somatostatin), which has been recently isolated from ovine hypothalamic extracts and also exhibits enhanced growth hormone release-inhibiting activity (*7*).

The relative concentrations of somatostatin-14 and the 3000- and ≥ 5000-dalton species in synaptosomes and those released by stimulation with 10 μ*M* ionophore A23187 or 100 m*M* KCl (Table 1) show that, relative to somatostatin-14, substantial quantities of the 3000-dalton species are released from synaptosomes. Furthermore, since the cross-reactivity of octacosa somatostatin with the antiserums used is low, these values were an underestimate of the mass of the released 3000-dalton species. On a molar basis, approximately 0.8 and 5 times as much 3000-dalton somatostatin as somatostatin-14 is released by stimulation with KCl and ionophore A23187, respectively (Table 1). Since the growth hormone release-inhibiting activity of octacosa somatostatin and somatostatin-25 is 1 to 14 times that of somatostatin-14 on a molar basis (*6, 7, 9*), the total bioactivity released as the 3000-dalton species could be even greater than that secreted as somatostatin-14. Thus, in vivo, the secreted 3000-dalton species potentially exert a greater regulating influence on growth hormone secretion than somatostatin does.

Our findings demonstrate that, in addition to somatostatin-14, immunoreactive species of 3000 daltons (which include octacosa somatostatin) and a species of 5000 daltons or more are present in synaptosomes isolated from ovine stalk median eminences. Moreover, both somatostatin-14 and the octacosa species are released from these synaptosomes by 100 m*M* KCl or by the calcium ionophore A23187, agents known to stimulate somatostatin secretion from synaptosomes in a physiologically meaningful manner (*8, 11*).

Octacosa somatostatin is thought to be a prohormonal form of somatostatin-14 (*5, 6*). It has also been postulated that somatostatin-14 is a biologically active fragment of a larger molecule of greater specific activity, rather than octacosa somatostatin being a precursor of the tetradecapeptide (*7*). In all probability, octacosa somatostatin has both a hormonal and prohormonal role. Our finding that somatostatin-14 and octacosa somatostatin occur in and are secreted from stalk median eminence nerve endings points to a biological function for both forms. The existence of at least two biologically active secreted forms of somatostatin suggests that there may be subtle differences, yet to be elucidated, in the regulatory function of the two peptides.

C. F. KEWLEY
R. P. MILLAR
M. C. BERMAN
Medical Research Council Biomembrane Unit, Department of Chemical Pathology, University of Cape Town, Observatory 7925, South Africa
A. V. SCHALLY
Endocrine and Polypeptide Laboratories, Veterans Administration Hospital, New Orleans, Louisiana 70112

References and Notes

1. P. Brazeau, W. Vale, R. Burgus, N. Ling, M. Butcher, J. Rivier, R. Guillemin, *Science* **179**, 77 (1973).
2. A. V. Schally, A. Dupont, T. W. Redding, G. L. Linthicum, *Fed. Proc. Fed. Am. Soc. Exp. Biol.* **35**, 584 (1975); W. Vale, N. Ling, J. Rivier, J. Villarreal, C. Rivier, C. Douglas, M. Brown, *Metab. Clin. Exp.* **25**, 1491 (1976); R. P. Millar, *J. Endocrinol.* **77**, 429 (1978); M. Lauber, M. Camier, P. Cohen, *Proc. Natl. Acad. Sci. U.S.A.* **76**, 6004 (1979); E. S. Zyznar, J. M. Conlon, V. Schusdziarra, R. H. Unger, *Endocrinology* **105**, 1426 (1979); L. Pradayrol, J. A. Chavialle, M. Carlquist, V. Mutt, *Biochem. Biophys. Res. Commun.* **85**, 701 (1978); B. D. Noe, D. J. Fletcher, J. Spiess, *Diabetes* **28**, 724 (1979).
3. O. P. Rorstad, J. Epelbaum, P. Brazeau, J. B. Martin, *Endocrinology* **105**, 1083 (1979).
4. J. Spiess and W. Vale, *Biochemistry* **19**, 2861 (1980).
5. L. Pradayrol, H. Jornvall, V. Mutt, A. Ribet, *FEBS Lett.* **109**, 55 (1980).
6. A. V. Schally *et al.*, *Proc. Natl. Acad. Sci. U.S.A.* **77**, 4489 (1980).
7. P. Brazeau, N. Ling, F. Esch, P. Bohlen, R. Benoît, R. Guillemin, *C.R. Acad. Sci. Ser. D* **290**, 1369 (1980).
8. C. F. Kewley, R. P. Millar, M. C. Berman, in *Neuropeptides: Biochemical and Physiological Studies*, R. P. Millar, Ed. (Churchill Livingstone, Edinburgh, 1981), pp. 78–86.
9. C. A. Meyers, W. A. Murphy, T. W. Redding, D. H. Coy, A. V. Schally, *Proc. Natl. Acad. Sci. U.S.A.* **77**, 6171 (1980).
10. S. Kronheim, M. Berelowitz, B. L. Pimstone, *Clin. Endocrinol. (Oxford)* **5**, 619 (1976).
11. I. Wakabayashi, Y. Miyazowa, M. Kanda, N. Miki, R. Demura, H. Demura, K. Shizume, *Endocrinol. Jpn.* **24**, 601 (1978); G. W. Bennett, J. A. Edwardson, D. Marcano de Cotte, M. Berelowitz, B. L. Pimstone, S. Kronheim, *J. Neurochem.* **32**, 1127 (1979); M. C. Sheppard, in *Neuropeptides: Biochemical and Physiological Studies*, R. P. Millar, Ed. (Churchill Livingstone, Edinburgh, 1981), pp. 98–103.
12. Supported by grants from the Medical Research Council of South Africa, the Harry Crossley Foundation, and the Merrin Bequest. We thank A. Arimura, W. Vale, and S. Kronheim for somatostain antiserums and E. Goddard and W. Gevers for their help and advice.

12 November 1980; revised 17 February 1981

Single Neostriatal Efferent Axons in the Globus Pallidus: A Light and Electron Microscopic Study

Abstract. *Intracellularly labeled rat neostriatal projection neurons were analyzed with both light and electron microscopy. The axons of medium spiny neurons were traced into the globus pallidus and were found to make synaptic contacts with pallidal dendrites. Despite the common somato-dendritic morphology of the neostriatal projection neurons, two different distribution patterns of efferent axons were observed, indicating the presence of functionally different medium spiny neurons in the neostriatum.*

Intracellular labeling techniques combined with intracellular recording allow direct correlative analysis of structure and function of individual neurons (*1*). Traditional classification of neurons, based on morphological characteristics, may now be correlated with physiological properties as determined by intracellular recording. For example, it has been demonstrated that neostriatal projection neurons receive convergent excitatory extrinsic inputs and when labeled with intracellular horseradish peroxidase (HRP), these cells were identified as medium spiny neurons (*2*). The HRP labeling not only revealed the characteristic somato-dendritic morphology of these neurons, which have been described in Golgi studies (*3*), but also enable serial reconstruction of the elaborate arborizations of their intrinsic axon collaterals (*4*). Detailed electron microscopic observations of the somata, dendrites, and intrastriatal connections of these neurons have also been described (*5*). We report that these medium spiny neurons may be further subdivided on the basis of differences in extrinsic axon distribution patterns. We also analyzed the synaptic contacts and postsynaptic targets of individually labeled striopallidal axons by electron microscopy.

Following intracellular recordings, rat neostriatal neurons were labeled by intracellular iontophoretic injections of HRP, fixed, and processed histochemically. Sections containing neostriatum and globus pallidus (GP) were analyzed by both light and electron microscopy (*6*).

All of the neostriatal projection neurons identified in this study were medi-

0036-8075/81/0821-0915$00.50/0

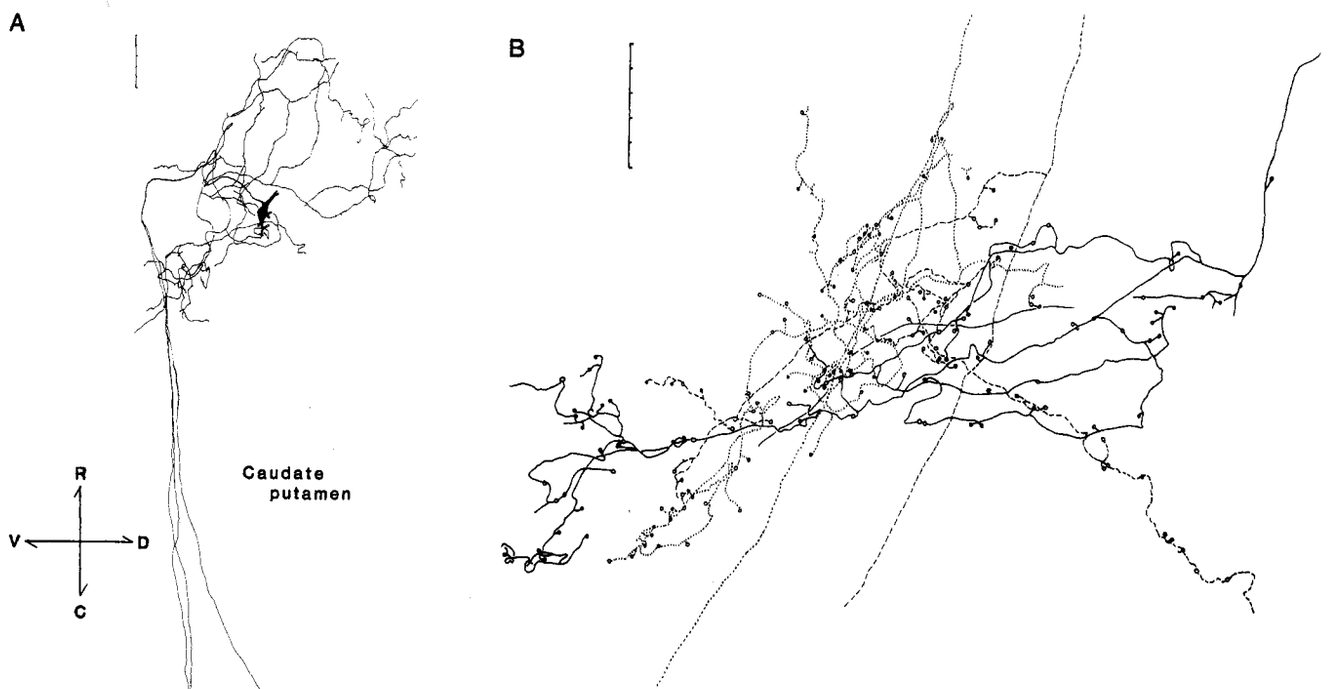

Fig. 1. (A) Reconstruction of the axonal distribution of an identified striopallidal neuron of the type exhibiting intrastriatal branching of the main axon and profuse pallidal arborization. The dendrites are omitted from the tracing to clarify the distribution of local axon collaterals. Note the presence of two discrete terminal fields in the globus pallidus. (B) A higher magnification drawing of the rostral terminal field in the GP from the neuron in (A). The three main axonal branches are shown as solid, dashed, and dotted lines so that the extent of overlap of their terminal fields is apparent. Scale bars, 50 μm. *R*, rostral; *C*, caudal; *V*, ventral; *D*, dorsal.

um spiny neurons and were identified on the basis of their somato-dendritic morphology. They had spine-free somata and primary dendrites and heavily spine-laden secondary and higher order dendritic branches. This result agrees well with studies showing that medium spiny neurons are neostriatal efferent cells (*4*, *7*). However, they could be divided into two distinct groups according to their efferent axonal morphology, such as their pattern of projection to GP.

In both groups of neurons, the main axon emitted several local collaterals in the striatum to form a complex arborization near the dendritic domain of the neuron of origin. In one group of cells ($N = 7$), the main efferent axons were unbranched throughout their course in the neostriatum and gave rise to either none or only one or two thin collateral fibers along their course in the GP. These observations are in agreement with a light microscopic study of striopallidal axons (*4*). The main axons did not end in the GP but coursed caudally into the internal capsule. Some of the collateral fibers in the GP became beaded, resembling "boutons en passant," but no elaborate axonal arborizations were seen. The HRP reaction product within the thin collateral fibers often faded quickly beyond detection a short distance from the main axons.

Electron microscopic analysis revealed that the main axons of these cells were thinly myelinated throughout their course in the neostriatum and the GP and that collateral fibers within the GP were unmyelinated. Some of these neostriatal projection neurons responded antidromically after stimulation of the substantia nigra, a known neostriatal target area distal to the GP. These results indicate that some striatal neurons project to both the GP and the substantia nigra.

In another group of neostriatal projection neurons ($N = 6$), the main axons divided within the neostriatum into two or three primary branches that descended in parallel courses toward the GP (Figs. 1A and 2A). Branching occurred either close to the soma or within the fiber bundles of the internal capsule. Upon entering the GP, these branches immediately gave rise to very localized but highly elaborate and overlapping axonal arborizations in the rostral GP (Fig. 1B). Some primary axonal branches ended at this area, but others continued caudally and then formed another separate collateral arborization in the caudal GP. These axon arborizations again overlapped extensively. In one case (Fig. 1), a primary branch continued caudally beyond the GP into the internal capsule, where the HRP labeling became too faint to be traced any further. The

intrinsic axonal collateral arborization in the neostriatum and the terminal axonal arborizations in both the rostral and the caudal GP appeared to be similar in size (~ 400 μm in diameter). Electron microscopic analysis revealed that these axons were thinly myelinated before branching in the neostriatum but were unmyelinated after branching.

Although all neurons of the second group had the same basic pattern of axonal arborizations, the locations of the terminal fields in the GP appeared to vary with the location of the neuron of origin in the neostriatum. That is, more medially placed neostriatal cells gave rise to more medially placed fields in the GP, and dorsally placed neurons arborized more dorsally in the GP. This result agrees well with studies of the topographical organization of the neostriatal efferent system (*8*). However, no indication of a rostrocaudal organization was obtained, since all adequately labeled neurons of this group showed both rostral and caudal terminal fields in the GP. No apparent differences were observed in the spatial distribution of the cell bodies of these two groups of medium spiny neurons in the neostriatum.

The neostriatal efferent axonal arborization in the GP consisted of thin unmyelinated fibers and boutons of both the en passant and terminaux types (Figs. 1B and 2B). These boutons, containing large and moderately pleomorphic vesicles (Fig. 2C), formed symmetrical synaptic junctions with pallidal dendrites of all sizes, including the occasional dendritic spines found on some dendrites (Fig. 3). Most of the synapses were formed with the small and medium-sized dendrites that predominate in the neuropil of the GP. The ultrastructure of these HRP-labeled boutons in the GP appeared to be identical to the labeled intrinsic terminals of medium spiny neurons in the neostriatum (*5*). They are also similar to those that have been described as neostriatal efferent terminals from degeneration studies in the cat (*9*) and the monkey (*10*).

Analysis of serial thin sections through individual boutons showed that every labeled bouton formed only one synapse with one postsynaptic element. Two or more labeled boutons, however, arising from the same axon collateral often contacted the same pallidal dendrite, thus confirming a degree of the longitudinal axodendritic organization of the striopallidal connections as postulated from light microscopic analysis of Golgi impregnated material (*11*). But even in areas of their highest density, as shown reconstructed from light microscopic drawings (Fig. 1B), the labeled boutons represented only a minute fraction of the total number of boutons with similar striopallidal morphology, thus indicating a high degree of convergence of neostriatal axons upon pallidal neurons.

A single neostriatal medium spiny neuron could also exert divergent influences on many GP neurons through its large terminal axonal plexus. Since most GP neurons have dendrites that are longer than the diameter of the terminal axonal arborization of any single neostriatal efferent neuron (*12*), it is probable that many GP neurons whose somata are outside of a particular terminal axonal arborization will receive direct axodendritic synaptic contacts from that neo-

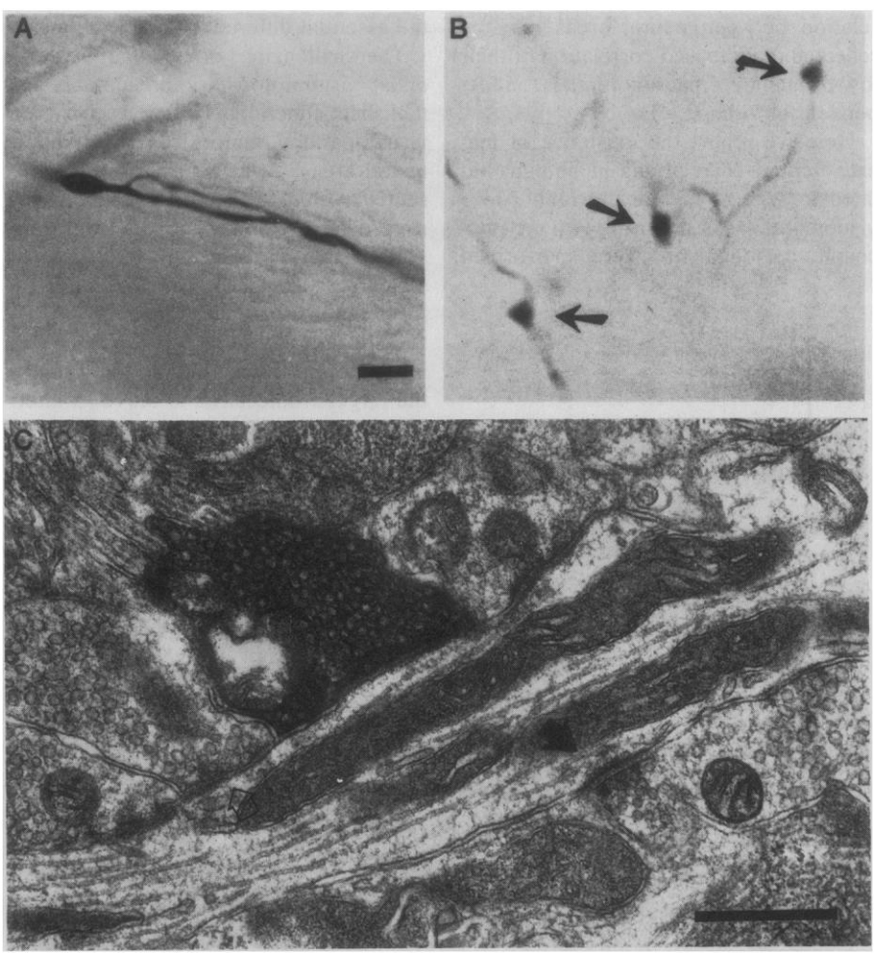

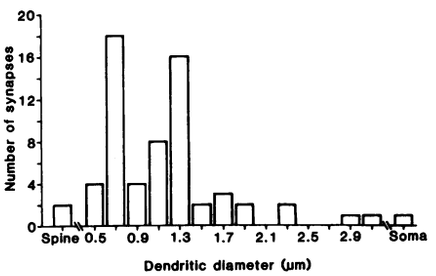

Fig. 2 (left). (A) Photomicrograph of the first branching of the main axon of the neuron shown in Fig. 1. Although the branch forms at right angles to the parent axon, it immediately turns to take a parallel course toward the GP. The varicosity near the branch point was not presynaptic. Scale bar, 2 μm. (B) Photomicrograph of a portion of a terminal arborization formed in the GP by an intracellularly stained striopallidal neuron. Arrows indicate the positions of electromicroscopically identified presynaptic boutons such as the one shown in (C). Magnification as in (A). (C) Electron micrograph of a presynaptic bouton from an intracellularly stained axon of a striopallidal neuron. The postsynaptic element is a small pallidal dendrite that also received several unlabeled presynaptic boutons. Some of these (open arrow) exhibit morphology similar to that of the labeled terminal, while others (solid arrow) contain smaller and more uniform synaptic vesicles and form synaptic contacts with more pronounced postsynaptic densities. Scale bar, 0.5 μm. Fig. 3 (above). Distribution of postsynaptic elements involved in a sample of 64 striopallidal synapses formed by intracellularly stained neurons. Dendritic diameters were measured from single sections at the site of contact with the labeled axon terminals; for obliquely sectioned dendrites, measurements were taken perpendicular to the axis of elongation as indicated by the orientation of microtubules. Most synapses were formed on small dendritic shafts less than 2 μm in diameter, although all areas of somatodendritic membrane of pallidal neurons could receive striopallidal synapses.

striatal projection neuron. Therefore, the field of influence of any particular efferent neuron at its target nuclei, as defined by the position and the extent of its terminal arborizations, must take synaptic contacts on long dendrites into consideration. Neurons with cell bodies outside of an apparent afferent terminal field still could be directly influenced by that afferent source.

Our results also show that even though all of the identified neostriatal efferent neurons are medium spiny neurons, the distribution of their main axons could be very different. This demonstrates that neurons with similar somato-dendritic morphology that receive similar afferent inputs can have different projection patterns and thus differ considerably in function.

H. T. CHANG
C. J. WILSON, S. T. KITAI
Department of Anatomy, Michigan State University, East Lansing 48824

References and Notes

1. P. J. Snow, P. K. Rose, A. G. Brown, *Science* **191**, 312 (1976); S. Cullheim and J. O. Kellerth, *Neurosci. Lett.* **2**, 307 (1976); E. Jankowska, J. Rastad, J. Westman, *Brain Res.* **105**, 557 (1976).
2. S. T. Kitai, J. D. Kocsis, R. J. Preston, M. Sugimori, *Brain Res.* **109**, 601 (1976).
3. J. M. Kemp and T. P. S. Powell, *Philos. Trans. R. Soc. London Ser. B* **262**, 383 (1971); C. A. Fox, A. N. Andrade, D. E. Hillman, R. C. Schwyn, *J. Hirnforsch.* **13**, 181 (1971–1972); M. DiFiglia, P. Pasik, T. Pasik, *Brain Res.* **114**, 245 (1976).
4. R. J. Preston, G. A. Bishop, S. T. Kitai, *Brain Res.* **183**, 253 (1980).
5. C. J. Wilson and P. M. Groves, *J. Comp. Neurol.* **194**, 599 (1980); G. A. Bishop. H. T. Chang, S. T. Kitai, *Soc. Neurosci. Abstr.* **5**, 67 (1979); H. T. Chang, G. A. Bishop, S. T. Kitai, *ibid.*, p 69.
6. Intracellularly recorded striatal neurons were labeled with HRP by passage of 2 to 5 nA (300 msec duration, 50 percent duty cycle) of positive ejection pulses through recording electrodes filled with 4 percent HRP in 0.05*M* tris-HCl buffer (*p*H 7.6) and 0.5*M* potassium chloride or potassium methylsulfate. Rat brains were fixed by intracardial perfusion of buffered Ringer solution followed by a solution of 2 percent formaldehyde and 2 percent glutaraldehyde in 0.15*M* phosphate buffer (*p*H 7.4). Survival periods following intracellular labeling ranged from 2 to 6 hours. Serial vibratome sections were cut in the sagittal plane and processed for light and electron microscopic analysis as described by C. J. Wilson and P. M. Groves [*J. Neurosci. Methods* **1**, 383 (1979)]. With frequent light microscopic examination of the block face during thin sectioning, individual axons and boutons were identified by both light and electron microscopy.
7. P. Somogyi and A. D. Smith, *Brain Res.* **178**, 3 (1979).
8. I. Grofova, in *The Neostriatum*, I. Divac and R. G. E. Oberg, Eds. (Pergamon, Oxford, 1979), pp. 37–52.
9. J. M. Kemp, *Brain Res.* **17**, 125 (1970); I. Grofova and E. Rinvik, *Exp. Brain Res.* **11**, 249 (1970).
10. C. A. Fox, J. A. Rafols, W. M. Cowan, *J. Comp. Neurol.* **159**, 201 (1975).
11. C. A. Fox and J. A. Rafols, *ibid.*, p. 177.
12. Unpublished observations (W. Falls, M. R. Park, S. T. Kitai) on both intracellularly labeled GP neurons and Golgi impregnated material indicate that most GP neurons in the rat have dendrites extending up to 1 mm away from the soma.
13. We thank B. Bitzinger and C. Meister for their skillful assistance in photograph and manuscript preparations. This study was supported by Public Health Service grant NS 14866 to S.T.K. and NS 17294 to C.J.W.

16 December 1980; revised 17 February 1981

Electrical Potentials in Human Brain During Cognition: New Method Reveals Dynamic Patterns of Correlation

Abstract. *A new technique has been developed for identifying, in humans, dynamic spatiotemporal electrical patterns of the brain during purposive behaviors. In this method, single-trial time-series correlations between brain macropotentials recorded from different scalp sites are analyzed by distribution-independent mathematical pattern recognition. Dynamic patterns of correlation clearly distinguished two brief visuomotor tasks differing only in type of mental judgment required (spatial or numeric). These complex patterns shifted in the anterior-posterior and left-right axes between successive 175-millisecond intervals, indicating that many areas in both cerebral hemispheres were involved even in these simple judgments. These patterns were not obtainable by conventional analysis of averaged evoked potentials or by linear analysis of correlations, suggesting that the new technique will advance the study of human brain activity related to cognition and goal-directed behaviors.*

The use of correlation measures of brain macropotentials, recorded as electroencephalogram (EEG) time series, for studying mass neural processes related to purposive behaviors (*1–3*) is based on the hypothesis that during purposive behaviors in humans many cortical and subcortical areas are functionally related (*4*). Although the means of communication between these areas and the relation of such communication to macropotentials are not well understood (*5*), there is evidence that increasing functional interrelation between neural areas may be reflected in increased correlation of their low-frequency macropotentials, independent of voltage (*6*).

Here we report the existence of macropotential correlations in humans related to type of mental judgment. Two visuomotor tasks requiring two types of cognitive judgment were performed while a high degree of control over stimulus-, response-, and performance-related factors was maintained. Small differences in patterns of correlation between tasks were extracted by applying distribution-independent mathematical pattern recognition, without signal averaging which obscures the individual-trial interareal phase relations. The results show spatially and temporally differentiated patterns of correlation delineating both the time course of mass neural processes associated with each task and the essential differences between tasks.

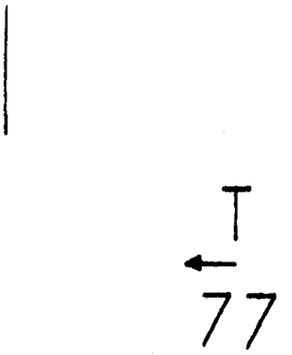

Fig. 1. Typical stimulus for arrow and number tasks. The stimulus subtended less than 2° visual angle. The participant was instructed either to produce a force which would cause the target (vertical line at left) to intersect the arrow's projection or to produce a force corresponding to the magnitude of the number, by a graded isometric contraction of the index finger. Differences in accuracy and response time were equalized between tasks by on-line computer adjustment of difficulty. Thus the two different cognitive tasks had the same stimuli, were performed equally well, and had the same response. Average response time was 1.2 seconds.

The challenging, brief (about 1.2 seconds) visuomotor task presumably established functional relations between visual, parietal, motor, frontal, and other neural areas. After a task cue was presented, a simple visual stimulus (an arrow, a target, and a number) was presented (Fig. 1) requiring a judgment of magnitude. The response was to exert a force on an isometric transducer with a ballistic contraction of the right index finger, proportional either to the distance the target would have to move to intersect the arrow's projection, or to the magnitude of the number (on a scale of 1 to 100). Arrow and number stimuli were always presented together, and the participant was task-cued in randomly ordered blocks of 13 trials (*7*). Performance-related factors were equalized between tasks by computer-controlled, on-line adjustment of the target size (arrow task) and the accuracy tolerance (number task) (*8*).

Five clinically normal, right-handed adults (four males, one female) each performed a total of about 270 trials. Sixteen electrodes were placed according to standard skull landmarks in positions covering the cranium (*9*). Vertical and horizontal eye movements, flexor muscle activity of the right index finger, and the resultant output of the isometric force transducer were recorded.

For each person, sets of trials of each

0036-8075/81/0821-0918$01.00/0